Thin Solid Films 634 (2017) 165–168

Contents lists available at ScienceDirect

Thin Solid Films

journal homepage: www.elsevier.com/locate/tsf

MgZnO based ultraviolet photodetector with high photoresponsivity achieved by fluorine doping

Yaonan Hou [a], Zengxia Mei [a,*], Zhanglong Liu [a], Huili Liang [a], Changzhi Gu [a], Xiaolong Du [a,b,**]

[a] Beijing National Laboratory for Condensed Matter Physics, Institute of Physics, Chinese Academy of Sciences, Beijing 100190, China
[b] School of Physical Sciences, University of Chinese Academy of Sciences, Beijing 100190, China

ARTICLE INFO

Article history:
Received 7 November 2016
Received in revised form 24 March 2017
Accepted 28 March 2017
Available online 3 April 2017

Keywords:
Magnesium zinc oxide
Photodetectors
Metal-semiconductor-metal
Schottky barrier
Fluor doping

ABSTRACT

We report a high-responsivity ultraviolet photodetector fabricated from fluorine doped $Mg_{0.4}Zn_{0.6}O$ thin film grown by molecular beam expitaxy. The doped epitaxial film demonstrates a low resistivity with a carrier concentration of 2.18×10^{17} cm^{-3} and mobility of 2.67 $cm^2/V\,s^{-1}$ by Van der Pauw Hall measurements. With a further study of a single Ti/Au-MgZnO:F Schottky junction, it is found the device has a lowered barrier height of 0.59–0.64 eV compared with the calculated value. Our photodetector configured with a metal-semiconductor-metal structure with Ti/Au interdigital electrodes exhibits a high photoresponsivity of 80 A/W, nearly 800 times larger than that of undoped sample. This record-high value is attributed to the lowered Schottky barrier as well as reduced barrier thickness thanks to the effective fluorine doping.

1. Introduction

ZnO and MgZnO alloys have attracted much attention for the past two decades due to their multifunctional applications [1–5]. Because of their unique optical properties such as large exciton binding energy of 60 meV at room temperature, high optical gain, [6] and good radiation hardness [7], they are ideal semiconductors for high-performance photonic devices which are able to work under extreme environments. The tunable band gap of $Mg_xZn_{1-x}O$ alloy (from 3.4 eV up to 7.8 eV) further enables the manipulation of working wavelengths in a broad range in the electromagnetic spectrum, for instance, multi-wave band ultraviolet (UV) photodetectors (PDs) [8,9]. Due to the strong ionic bonding between Mg and O atoms, the high resistance of $Mg_xZn_{1-x}O$ particularly with high Mg content hampers the practical applications of such devices, especially in modern high-speed circuits. One of the most straightforward and effective approaches to reducing its resistance is doping. Generally, n-type doping of $Mg_xZn_{1-x}O$ is achieved by substituting cations of Mg^{2+} or Zn^{2+} atoms with group-III ions, such as B^{3+}, Al^{3+}, Ga^{3+}, and In^{3+} [10–13]. However, it is found the ionization efficiency of such dopants is becoming less impressive with increasing Mg content (or band gap), highly likely due to the less changeable doping level depth with respect to the significantly elevated conduction band minimum dominated by Mg's 3s electrons.

Based on the breakthroughs in synthesis of high-quality $Mg_xZn_{1-x}O$ epitaxial films with high Mg contents, our group solved the doping problem by alternatively substituting O^{2-} with fluorine anions, F^- [14]. The resistance was effectively reduced to ~10^2 Ω·cm compared with ~10^6 Ω·cm of the undoped films with the Mg content up to 51%. However, the influences of doping on the performance of UV PDs have not been well studied till now. In this work, we present a systematic study of a metal-semiconductor-metal (MSM) UV PD fabricated from an effectively F-doped $Mg_{0.4}Zn_{0.6}O$ epitaxial film grown by radio-frequency plasma-assisted molecular beam expitaxy (rf-MBE). The device exhibits a huge photo-responsivity of ~80 A/W at a 2 V external bias, without damaging the transient response properties. Our results unambiguously reveal that the performance of the UV PD can be massively enhanced by F doping.

2. Experiments

Our MgZnO:F thin film was grown on a c-plane sapphire substrate by rf-MBE equipped with an *in situ* reflection high-energy electron diffraction (RHEED) to monitor the growth situations. Before loading to the growth chamber, the substrate underwent a standard chemical cleaning by using boiling acetone and ethanol. Then 750 °C thermal cleaning and reactive oxygen radical treatment were performed before growth, after which bright diffraction patterns of the sapphire substrate were observed through RHEED (Fig. 1a). Following that an ultrathin MgO layer (<1 nm) was deposited at 500 °C as a template for the growth of wurtzite MgZnO [15]. Subsequently, a thin MgZnO layer with a relatively low Mg content was grown as "quasi-homo" buffer,

* Corresponding author.
** Correspondence to: X. Du, Beijing National Laboratory for Condensed Matter Physics, Institute of Physics, Chinese Academy of Sciences, Beijing 100190, China.
E-mail addresses: zxmei@iphy.ac.cn (Z. Mei), xldu@iphy.ac.cn (X. Du).

http://dx.doi.org/10.1016/j.tsf.2017.03.054
0040-6090/

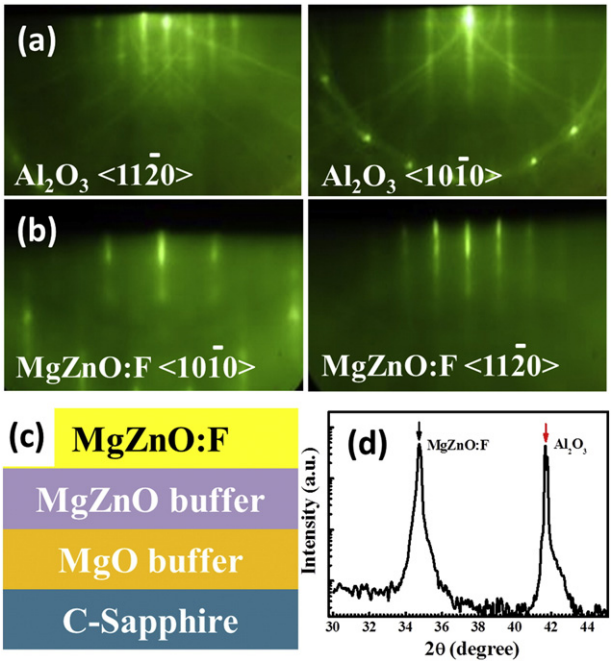

Fig. 1. RHEED observations of the sapphire substrate after oxygen treatment (a) and the grown $Mg_{0.4}Zn_{0.6}O$:F film (b). (c) Schematic structure of the epitaxial film. (d) XRD θ–2θ scan of $Mg_{0.4}Zn_{0.6}O$:F film.

on which the $Mg_{0.4}Zn_{0.6}O$:F was eventually grown at 450 °C. During the growth, high-purity ZnF_2 was used as the doping source evaporated from a Knudsen-cell at 390 °C while keeping the II/VI ratio of 9/5. At this temperature, the doping concentration is estimated to be 2.48 × 10^{17}/cm^3 by comparing with the pressure of ZnF_2 with the known value at 420 °C from our experiences [14]. The oxygen plasma flow rate and RF power were set at 2.6 standard cubic centimeters per minute (sccm) and 340 W, respectively.

Fig. 1b shows the RHEED patterns of the $Mg_{0.4}Zn_{0.6}O$:F expitaxial layer, obtained from its ⟨10−10⟩ and ⟨11−20⟩ planes, respectively. The bright stripy features of the RHEED patterns indicate a high crystallinity and an atomically flat surface. X-ray diffraction (XRD) was carried out using Cu-Kα radiation (M18AHF) in a θ–2θ scanning mode to further characterize the structural properties of the F-doped epilayer. As shown in Fig. 1d, the peak situated at 34.74° is the signature of the diffraction from (0002) planes of MgZnO whilst the one at 41.7° is assigned to sapphire substrate. The Mg content is estimated to be 40%. The single XRD diffraction peak from epilayer indicates our $Mg_{0.4}Zn_{0.6}O$:F epitaxial film is a single crystal with wurtzite structure, which was further verified by XRD ϕ-scan curve from (101) planes showing a six-fold symmetry, consistent with the RHEED observations.

3. Results and discussion

Optical properties of our $Mg_{0.4}Zn_{0.6}O$:F sample were performed by transmittance and photoluminescence (PL) characterizations. The room temperature transmittance spectrum is shown in the blue curve in Fig. 2, where two absorption edges locate at 290 nm (4.28 eV) and 343 nm (3.62 eV), corresponding to the near band edge absorption of $Mg_{0.4}Zn_{0.6}O$:F epilayer and the MgZnO "quasi-homo" buffer, respectively. PL was characterized by using UV light with a wavelength at 250 nm from synchrotron radiation as excitation source, as shown in the green curve in Fig. 2. Two emission peaks situated at 294 and 350 nm are detected, consistent with the transmittance measurement results. Full width at half maximum of PL spectra of $Mg_{0.4}Zn_{0.6}O$:F exhibits 13.7 nm compared with 10.1 nm of the undoped sample (black curve). The slight broadening of the near band edge emission is owing

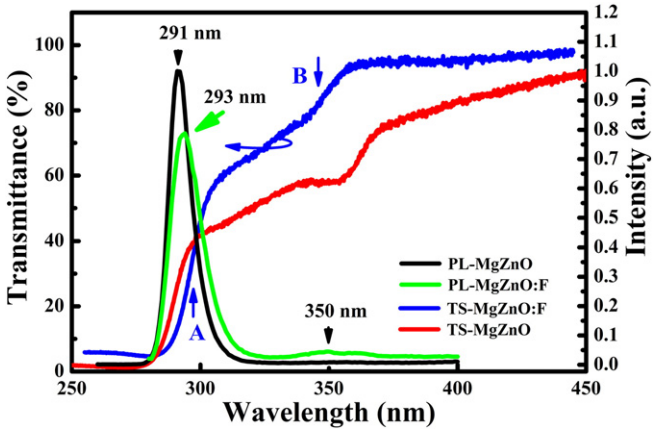

Fig. 2. PL (green curve) and transmittance (blue curve) spectra of $Mg_{0.4}Zn_{0.6}O$:F sample; the black and red curves shows the PL and transmittance of an undoped counterpart.

to the extended band tail states generated by doping. Overall, no strong degradation of optical property is observed by F doping.

The electrical property of our $Mg_{0.4}Zn_{0.6}O$:F film was initially characterized by Van der Pauw Hall measurement at room temperature. Carrier concentration and mobility are determined to be 2.18 × 10^{17}/cm^3, increased by >3 orders of magnitude compared with that of the undoped thin films (~10^{14} cm^{-3}). Considering the doping concentration, the activation efficiency of the dopants is 88%, suggesting F working as a shallow dopant in MgZnO [14]. Meanwhile, the mobility decreased from 4.63 to 2.62 $cm^2/V\cdot s$ due to F doping. In order to have a further insight into the electrical properties, we fabricated a pair of In-Ti/Au electrodes on our sample. The inset of Fig. 3a shows the In–In is a pair of good ohmic contacts, corroborated by the linear shaped current-voltage (I–V) curve. In contrast, the I–V scan of In-Ti/Au electrodes exhibits a clear rectification behaviour (Fig. 3a), indicating Schottky barrier forms at the Ti/$Mg_{0.4}Zn_{0.6}O$:F interface.

The typical I–V characteristics of Schottky barrier can be mathematically depicted by,

$$I = I_s[\ \exp(qV_b/nkT) - 1] \tag{1}$$

where $I_s = 1.335 \times 10^{-7}$ A is the reversed saturation current, V_b the applied bias and n the ideality factor. Among these parameters, the reversed saturation current is given by,

$$I_s = A^*T^2S\ \ \exp(-q\phi_{ms}/kT) \tag{2}$$

where A* is Richardson constant, which is estimated to be 32–48 $A\cdot cm^{-2}\cdot K^{-2}$ from that of ZnO and MgO [16,17]; S the contact area; ϕ_{ms} the barrier height of Schottky contact. From Eqs. (1) and (2), we obtained $n = 6.58$ and $\phi_{ms} = 0.59$–0.64 eV, respectively. The ideality factor deviating from 1 implies the carrier transportation mechanism is dominated by not only thermionic emission but also field emission. For the undoped sample, the barrier height estimated to be 0.74–0.97 eV, corresponding well with the one concluded from Schottky-Mott relation, $\phi_{ms} = \phi_m - \chi = 0.85$ eV (Fig. 3b), if the conduction band minimum and valence band maximum change according to the ratio of ΔE_c:ΔE_v = 9:1 by incorporation of Mg into ZnO [18]. The Schottky barrier height of our device is reduced by 0.21–0.26 eV compared with the ideal value. Furthermore, the Schottky barrier thickness (W_d) is depicted by,

$$W_d = [2\varepsilon_s/qN(\varphi_{bi} - V - kT/q)\ ]^{1/2} \tag{3}$$

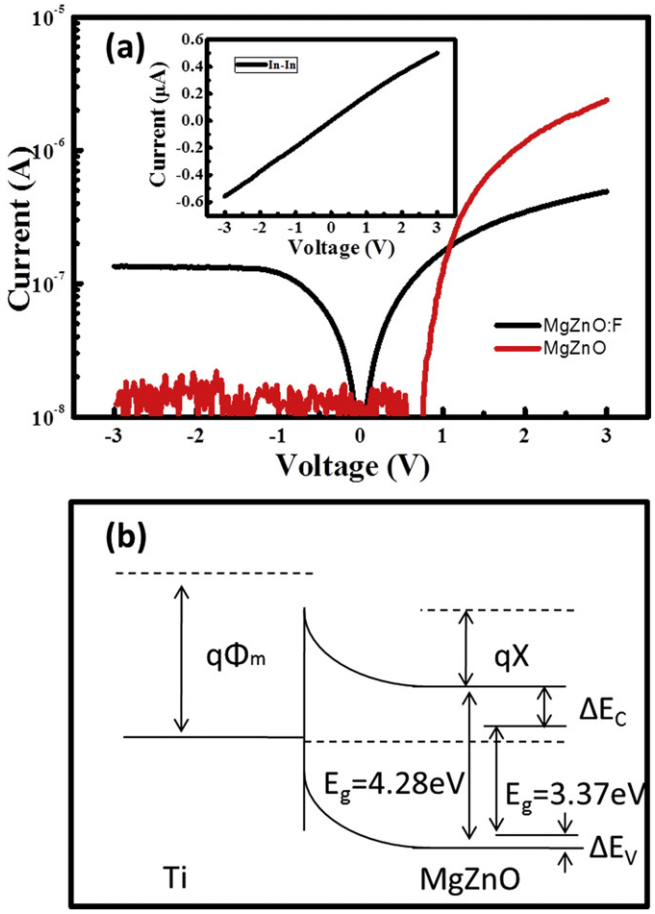

Fig. 3. (a) The I–V characteristics of In-$Mg_{0.4}Zn_{0.6}O$:F-Ti/Au Schottky diode and a reference device fabricated from undoped film; inset is the I–V curve of In-In contacts. (b) Schematic energy-band diagram of the Schottky barrier drawn according to Schottky-Mott relationship.

where ε_s, N and φ_{bi} are the dielectric constant, carrier concentration and built-in potential, respectively. With F doping, φ_{bi} decreases with the barrier height. Therefore, the barrier thickness reduces by >30 times with the carrier concentration increase by 3 orders of magnitude. Such a lowered barrier height along with a reduced thickness will enhance the photo-generated electrons transport from MgZnO to the electrode.

Our PDs were designed with interdigital MSM configuration, with the fingers 5 μm in width and 300 μm in length spaced by 5 μm gaps (inset of Fig. 4a). Ti/Au (10/50 nm) electrodes were deposited by thermal evaporation with background pressure of 5×10^{-4} Pa at a rate of 0.1 nm/s. For the sake of a direct comparison, we fabricated a reference sample with the identical structure from the undoped counterpart. Current-voltage (I—V) measurements were carried out by a Keithley 6487 picoammeter. As shown in Fig. 4b, the I–V curves of our PDs show highly symmetric rectifying behaviors, indicating a well-defined pair of back-to-back Schottky contacts. The saturation current of the undoped sample is ~10^{-9} A due to the huge resistance of intrinsic MgZnO film. In comparison, the saturation current of the doped sample increases to 5×10^{-8} A due to the reduced resistance as a result of F doping. On the other hand, a clear knee voltage at ~0.7 V (labeled by a black arrow in Fig. 4b) can be observed in the F doped sample; while it becomes obscure in the undoped sample, which shows a gradually increasing in the current. This is due to the rapidly expanding depletion region with the applied voltage resulting from the low carrier concentration in the undoped sample [19].

Spectral photoresponse measurements were performed with a 75 W Xe lamp combined with a monochromator with a focal length of 0.5 m as the excitation source, whilst the photocurrent at 2 V was recorded with a Keithley 2400 sourcemeter. As shown in Fig. 4c, both of the samples demonstrate a peak response at ~295 nm, consistent with the transmittance and PL results. The reference sample exhibits a responsivity ~0.1 A/W with a sharp cutoff situating at the band edge. In contrast, a very inclined response edge from 300 to 400 nm is identified from the spectral photoresponse of F doped sample, which is attributed to the band tail introduced by incorporation of F atoms [20]. In spite of this, the photo-responsivity (R) of the F-doped sample is as high as 80 A/W, 8×10^2 times larger than that of the undoped sample. The detectivity (D^*) of our device is determined to be $D^* = (A\Delta f)^{1/2} / NEP = 3.5 \times 10^8$ $Hz^{1/2}/W$, where the noise equivalent power is $NEP = (4k_BT / R_{dark} + 2qI_{dark})^{1/2}\Delta f^{1/2}/B$ (R_{dark}, I_{dark} and B are the differential resistance, dark current and bandwidth, respectively). Compared with our previous work on the photodetector fabricated from $Mg_{0.51}Zn_{0.49}O$:F [14], the detectivity decreased by an order of magnitude potentially due to the slow response.

The high photo-responsivity corresponds to a large external quantum efficiency (EQE) of 3.36×10^4%, obtained from EQE = 1240R/λ × 100%, suggesting a large photocurrent gain (G), which is potentially attributed to a combined effect of lowered Schottky barrier thickness/height (G_{sb}) and photoconductive gain (G_{ph}) due to F doping,

$$G = G_{sb} + G_{ph} \tag{4}$$

The photoconductive gain is in proportional to the mobility and photocarrier lifetime ($G_{ph} \propto \mu\tau$). Generally speaking, μ decreases with doping concentration as a result of enhanced electronic scattering, *e.g.* the mobility decreased from 4.63 for the undoped sample to 2.62 $cm^2/V{\cdot}s$ for the F doped sample. At the same time, it is observed τ increased by only ~2 by doping from the transient photocurrent measurement shown in the later section. In consequence, the contribution of G_{ph} to the whole photocurrent gain (G) is insignificant. On the other hand, Schottky barrier thickness decreases 30 times and height lowers by 0.21–0.26 eV as aforementioned reasons, which greatly enhances photogenerated carriers transporting through the barrier, leading to the huge response and the internal photocurrent gain.

Transient photoresponse measurement was carried out by illuminating the PD with a periodic (115 s) UV light with a wavelength at 254 nm as shown in Fig. 4d. The photocurrent drastically decreases at the time the UV light switches off. In order to study the details of the transient response, the photocurrent decay is fitted into a biexponential equation,

$$I(t) = I_1 \exp(-t/\tau_1) + I_2 \exp(-t/\tau_2) \tag{5}$$

where τ_1 and τ_2 are the fast and slow decay components, respectively. The former is related with the carriers directly recombining after light off, whilst the latter known as persistent photocurrent (PPC) is a slow recombination process normally mediated by defects, c.f. oxygen vacancies in ZnO based materials [21].Such slow response widely observed in wide band gap semiconductors based PDs hinders the devices from practical applications. In this work, the undoped sample shows a fast and slow decay time of 0.34 and 10 s (Fig. 4d), respectively. With F doping, the decay times increased to 0.61 and 12 s, respectively, indicating F doping will not introduce unexpected deep level defects causing a strong PPC problem.

4. Conclusion

In summary, effectively F-doped MgZnO film with a Mg content up to 40% has been readily achieved, with the carrier concentration and mobility of 2.17×10^{17} cm^{-3} and 2.67 $cm^2/V\ s^{-1}$, respectively. From the PL and transmittance measurements, no obvious deterioration of optical properties is introduced by F doping. Our PD designed with a metal-semiconductor-metal structure shows a huge responsivity of 80 A/W, ~800 times higher than that of undoped sample. The enhanced

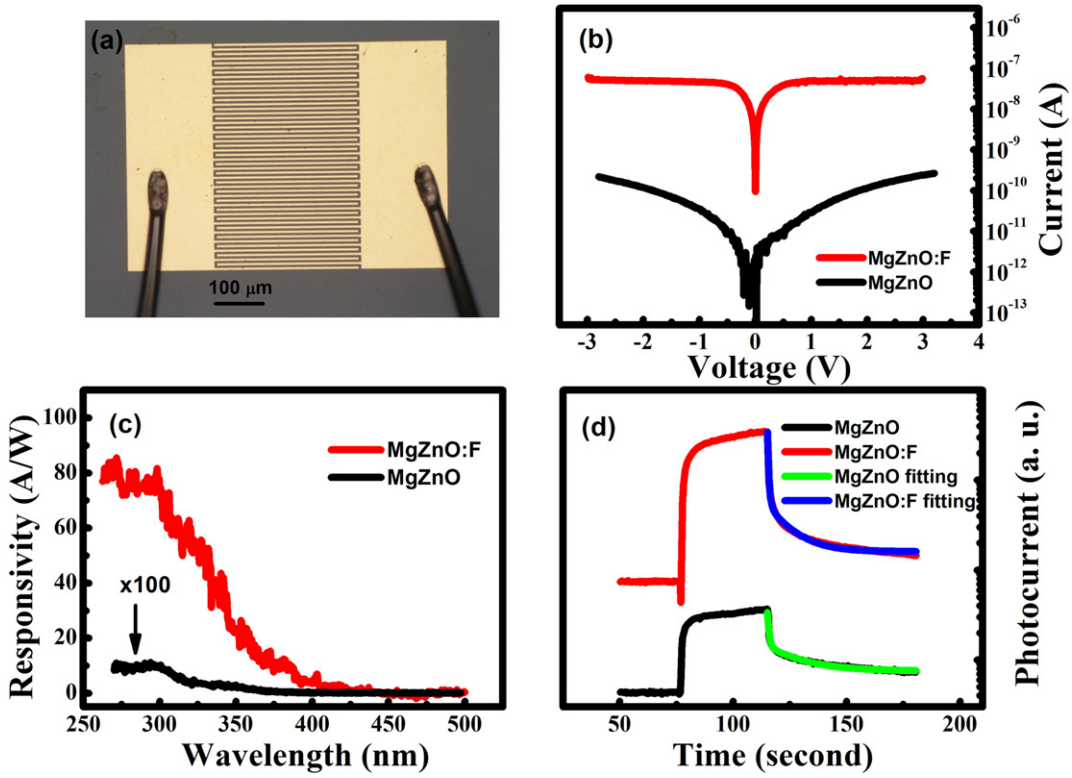

Fig. 4. (a) Photograph of the MSM PD obtained from an optical microscope (scale bar = 100 μm). (b) I–V curves of the MSM PD fabricated from the undoped (black) and F doped (red) sample. (c) The photoresponsivity of the PDs fabricated from the undoped (black) and F doped (red) sample. (d) Transient response of the PDs fabricated from the undoped (black) and F doped (red) sample.

responsivity is ascribed to the lowered barrier height of 0.59–0.64 eV as well as the reduced barrier thickness by 30 times due to F doping. From the transient response measurements, it is concluded F doping will not introduce deep level defects generating PPC problem.

Acknowledgements

This work was supported by the National Science Foundation (Grant nos. 11674405, 11274366, 61306011, 51272280, and 11675280), and the Diffusion Scattering Station in Beijing Synchrotron Radiation Facility.

References

[1] Y. Hou, Z. Mei, X. Du, Semiconductor ultraviolet photodetectors based on ZnO and $Mg_xZn_{1-x}O$, J. Phys. D. Appl. Phys. 47 (2014) 283001.
[2] M.A.M. Versteegh, D. Vanmaekelbergh, J.I. Dijkhuis, Room-temperature laser emission of ZnO nanowires explained by many-nody theory, Phys. Rev. Lett. 108 (2012) 157402.
[3] Z.L. Wang, J. Song, Piezoelectric nanogenerators based on zinc oxide nanowire arrays, Science 312 (2006) 242–246.
[4] R.L. Hoffman, B.J. Norris, J.F. Wager, ZnO-based transparent thin-film transistors, Appl. Phys. Lett. 82 (2003) 733.
[5] S.K. Arya, S. Saha, J.E. Ramirez-Vick, V. Gupta, S. Bhansali, S.P. Singh, Recent advances in ZnO nanostructures and thin films for biosensor applications: review, Anal. Chim. Acta 737 (2012) 1–21.
[6] J. Cui, S. Sadofev, S. Blumstengel, J. Puls, F. Henneberger, Optical gain and lasing of ZnO/ZnMgO multiple quantum wells: From low to room temperature, Appl. Phys. Lett. 89 (2006) 051108.
[7] K. Koike, T. Aoki, R. Fujimoto, S. Sasa, M. Yano, S. Gonda, R. Ishigami, K. Kume, Radiation hardness of single-crystalline zinc oxide films, Phys. Status Solidi C 9 (2012) 1577–1579.
[8] Y.N. Hou, Z.X. Mei, H.L. Liang, D.Q. Ye, C.Z. Gu, X.L. Du, Dual-band MgZnO ultraviolet photodetector integrated with Si, Appl. Phys. Lett. 102 (2013) 153510.
[9] Y.N. Hou, Z.X. Mei, H.L. Liang, C.Z. Gu, X.L. Du, Appl. Phys. Lett. 105 (2014) 133510.
[10] C. Avis, S.H. Kim, J.H. Hur, J. Jang, W.I. Milne, Coplanar ZnO thin-film transistor using boron ion doped source/drain contacts, Electrochem. Solid-State Lett. 12 (2009) J93–J95.
[11] T. Tsuboi, K. Yamamoto, A. Nakamura, J. Temmyo, Indium-doped $Mg_xZn_{1-x}O$ films for ZnO-based heterojunction diodes, Jpn. J. Appl. Phys. 49 (2010) 04DG13.
[12] Y. Sugimoto, K. Igarashi, S. Shirasaki, A. Kikuchi, Effect of Al doping in the Ag layer of MgZnO/Ag/MgZnO dielectric/metal/dielectric UV–visible transparent conductive films, Phys. Status Solidi C 13 (2016) 568–571.
[13] V. Awasthi, S.K. Pandy, V. Garg, B.S. Sengar, P. Sharma, S. Kumar, C. Mukherjee, S. Mukherjee, Plasmon generation in sputtered Ga-doped MgZnO thin films for solar cell applications, J. Appl. Phys. 119 (2016) 233101.
[14] L. Liu, Z. Mei, Y. Hou, H. Liang, A. Azarov, V. Venkatachalapathy, A. Kuznetsov, X. Du, Fluorine doping: a feasible solution to enhancing the conductivity of high-resistance wide bandgap $Mg_{0.51}Zn_{0.49}O$ active components, Sci. Rep. 5 (2015) 15516.
[15] X. He, L. Gu, S. Guo, Z. Liu, R. Yu, Z. Mei, X. Du, B. Liu, Y. Ikuhara, X. Duan, Oxygen polarity and interfacial atomic arrangement in an $Mg_xZn_{1-x}O$/C-MgO/sapphire heterostructure, J. Phys. D. Appl. Phys. 46 (2013) 145303.
[16] K. Sarpatwari, O.O. Awadelkarim, M.W. Allen, S.M. Durbin, S.E. Mohney, Extracting the Richardson constant: IrO_x/n-ZnOIrO_x/n-ZnO Schottky diodes, Appl. Phys. Lett. 94 (2009) 242110.
[17] A.F. Qasrawi, H.K. Khanfar, Current transport mechanism in Au-p-MgO-Ni Schottky device designed for microwave sensing, J. Optoelectron. Adv. Mater. 18 (2016) 639–644.
[18] A. Ohtomo, M. Kawasaki, I. Ohkubo, H. Koinuma, T. Yasuda, Y. Segawa, Structure and optical properties of ZnO/$Mg_{0.2}Zn_{0.8}O$ superlattices, Appl. Phys. Lett. 75 (1999) 980.
[19] M.Y. Chen, C.C. Chang, Monolithic integration of a ZnS MSM photodiode and an InGaP/GaAs HBT on a GaAs substrate, Semicond. Sci. Technol. 24 (2009) 045009.
[20] K.S. Ahn, Y. Yan, S. Shet, T. Deutsch, J. Turner, M. Al-Jassim, Enhanced photoelectrochemical responses of ZnO films through Ga and N codoping, Appl. Phys. Lett. 91 (2007) 231909.
[21] Y. Hou, Z. Mei, H. Liang, D. Ye, C. Gu, X. Du, Y. Lu, Annealing effects of Ti/Au contact on N-MgZnO/P-Si ultraviolet-B photodetectors, IEEE Trans. Electron Devices 60 (2013) 3474–3477.